

**MBE growth of highly sensitive silicon PIN diode with Magnetic GeMn quantum dots  
for optoelectronic applications**

**Mansour Aouassa<sup>1\*</sup>, Mohammed Bouabdellaoui<sup>2</sup>, Tarak Kallel<sup>1</sup>, Makrem Yahyaoui<sup>1</sup>,  
Thouraya Ettaghzouti<sup>1</sup>, Nouredine B. Afkir<sup>3</sup>, Abdulraoof Ali<sup>4</sup> and Ibrahim O.  
Althobaiti<sup>1</sup>**

<sup>1</sup>Department of Physics, College of Science and Arts, Jouf University, Al-Qurayat Branch, P.O.  
Box 756, Saudi Arabia.

<sup>2</sup>CNRS, Aix-Marseille Université, Centrale Marseille, IM2NP, UMR 7334, Campus de St. Jérôme, 13397  
Marseille, FRANCE.

<sup>3</sup>Laboratory of Physics of Condensed Matter and Renewable Energy, Faculty of sciences and technology,  
Hassan II University of Casablanca B.P 146, Mohammedia, Morocco.

<sup>4</sup>University of Pretoria Department of Physics, Hatfield, Pretoria, 0002, SOUTH AFRICA

**\*Corresponding author: Email: [maouassa@ju.edu.sa](mailto:maouassa@ju.edu.sa)**

**Abstract**

*This work reports for the first time the realization and the characterization of a p+-i-n+ diode based on magnetic GeMn quantum dots (p+-Si/i-Si:GeMn QDs/n+-Si) for photodetection and photovoltaic applications. The GeMn quantum dots are epitaxied by ultra-high vacuum molecular beam epitaxy (UHV-MBE) reactor on a silicon substrate. The results of morphological and magnetic characterizations obtained by atomic force microscopy and a superconducting quantum interference device show respectively that the GeMn QDs are homogeneous, dense, and ferromagnetic with a Curie temperature higher than room temperature ( $T_c=350$  K). The GeMn QD-based p+-i-n+ photodiode has a high rectification ratio of  $>100$  at a bias voltage  $V_b = \pm 1$  V, high-breakdown-voltage of 12V, an ideality factor  $n = 1.86$ , a Schottky barrier height  $\phi_B = 0.72$  eV and a broad spectral response in the visible with a high photocurrent/dark ratio of about 100. These original results pave the way for the real integration of GeMn-based magnetic quantum dots in advanced optoelectronic and spintronic applications.*

## 1. Introduction

For several years, magnetic semiconductors doped with elements IV and III-V ( $\text{Ge}_x\text{Mn}_{1-x}$ ,  $\text{Cr}_x\text{Ge}_{1-x}$ , Ni-GeSn, and their alloys) have been the subject of intense scientific research for their wide range of applications. Different components based on magnetic semiconductor nanostructures have been demonstrated, such as field effect transistors, light-emitting diodes, etc. [1-12]. As for diluted magnetic semiconductor quantum dots, their specific properties, such as the energy of their band gap, can be tuned to very short UV wavelengths (290 nm) by quantum confinement, and technological advancements in epitaxial growth techniques allow these quantum dots to be integrated into photodetectors and solar cells in order to maximize their performance [13]. The large lattice mismatch between GeMn alloys and commonly used substrates (Ge, Si, and SiC) presents a major challenge for the development of photodiodes based on thin films of GeMn. Indeed, stress relaxation leads to the formation of dislocations, which can have a density of the order of  $10^9 \text{ cm}^{-2}$ , which strongly degrades the efficiency of the device. Due to their small cross-section, GeMn quantum dots are a promising solution to the problem of dislocations since they can reduce stresses on the free lateral surface and eliminate dislocations. In addition, molecular beam epitaxy (MBE) allows the integration of GeMn quantum dots on cheap substrates such as silicon, which reduces the cost of development. It is now possible to grow devices based on GeMn quantum dots on a cheaper substrate such as silicon and take advantage of their excellent magnetic and opto-electrical properties. These types of structures are good candidates for the fabrication of new generations of nanopixel array photodetectors and solar cells.

In this article, we present the realization and characterization of a photodiode with GeMn quantum dots inserted in the intrinsic layer of a p<sup>+</sup>-i-n<sup>+</sup> junction epitaxially grown by MBE on a silicon substrate. The obtained electrical device characterizations of p<sup>+</sup>-Si/i-Si:GeMn

QDs/n<sup>+</sup>-Si structure show typical rectifier behavior of the p<sup>+</sup>-i-n<sup>+</sup> junction. The ideality factor  $n$ , the height of the barrier, and the series resistance were determined from the analysis of the current density versus voltage (J-V) characteristics using Cheung's method [14]. The influence of temperature on the J-V characteristic and the transport phenomena have been studied. The effects of interface states are also investigated using impedance spectroscopy. Photocurrent spectra were measured in the spectral range from UV to IR. They show that the spectral response is selective for photons with energy  $E > 1.12$  eV.

## 2. Technological process

The fabrication process of the GeMn quantum dots-based photodiode was carried out by molecular beam epitaxy (MBE) equipped with solid sources. The process includes the following steps:

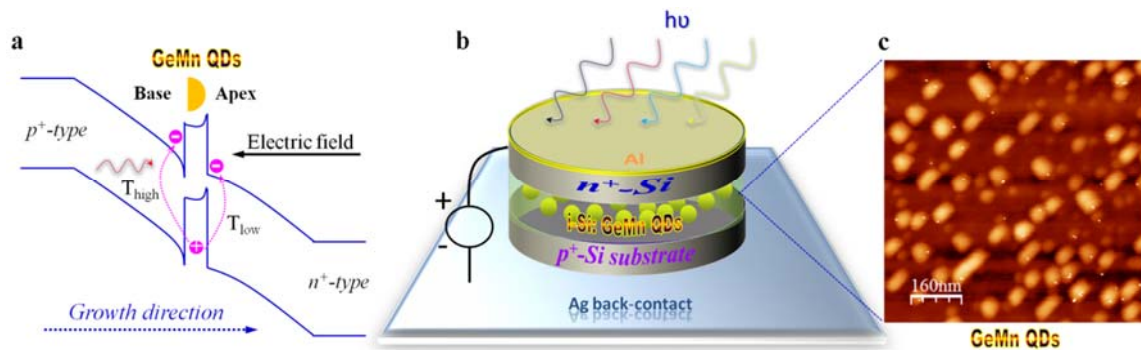
- 1) In-situ degassing of the p<sup>+</sup>-type silicon substrate (doping concentration =  $2 \times 10^{20} \text{ cm}^{-3}$ ) in the MBE reactor at 900 °C for 20 minutes, to remove any traces of oxide that formed after the RCA cleaning.
- 2) Growth of p<sup>+</sup>-type silicon film 400 nm thick (doping concentration =  $2 \times 10^{20} \text{ cm}^{-3}$ ) at a temperature of 520 °C.
- 3) Growth of a 1 nm-thick intrinsically crystalline silicon film at 350 °C.
- 4) Growth of GeMn quantum dots via the Stranski-Krastanov mode by depositing 2.5 nm of GeMn (Mn: 7%) at 350 °C.
- 5) Growth of an intrinsic crystalline silicon film 2 nm thick at 350 °C.
- 6) Growth of n<sup>+</sup>-type crystalline silicon 200 nm thick with a doping of  $2 \times 10^{20} \text{ cm}^{-3}$  at 350 C.
- 7) Deposition of a transparent contact by thermal evaporation of an aluminum layer 250 nm thick on the top of the sample, followed by a rapid thermal annealing at 350 °C

to improve the Al/Si interface.

### 3. Characterization

#### 3.1 Morphological characterization

Figures (1-a) and (1-b) show, respectively, the energetic diagram and a schematic representation of the fabricated p<sup>+</sup>-i-n<sup>+</sup> photodiode. Figures (1-c) and (1-d) show high- and low-magnification AFM images of self-assembled GeMn quantum dots grown on silicon using the Stranski-Krastanov growth mode and inserted into the intrinsic layer of a p<sup>+</sup>-i-n<sup>+</sup> diode, respectively. The quantum dots are very dense (density  $\sim 10^{10}$  cm<sup>-2</sup>) faceted, and oriented along the crystalline axis. The height profile along the line in (1-d) shown in figure (1-e) and the height distribution show that the GeMn QDs size varies between 0.5 and 3.5 nm. These properties indicate a strong quantum confinement in these quantum dots, which making them ideal for photovoltaic and photodetection applications.



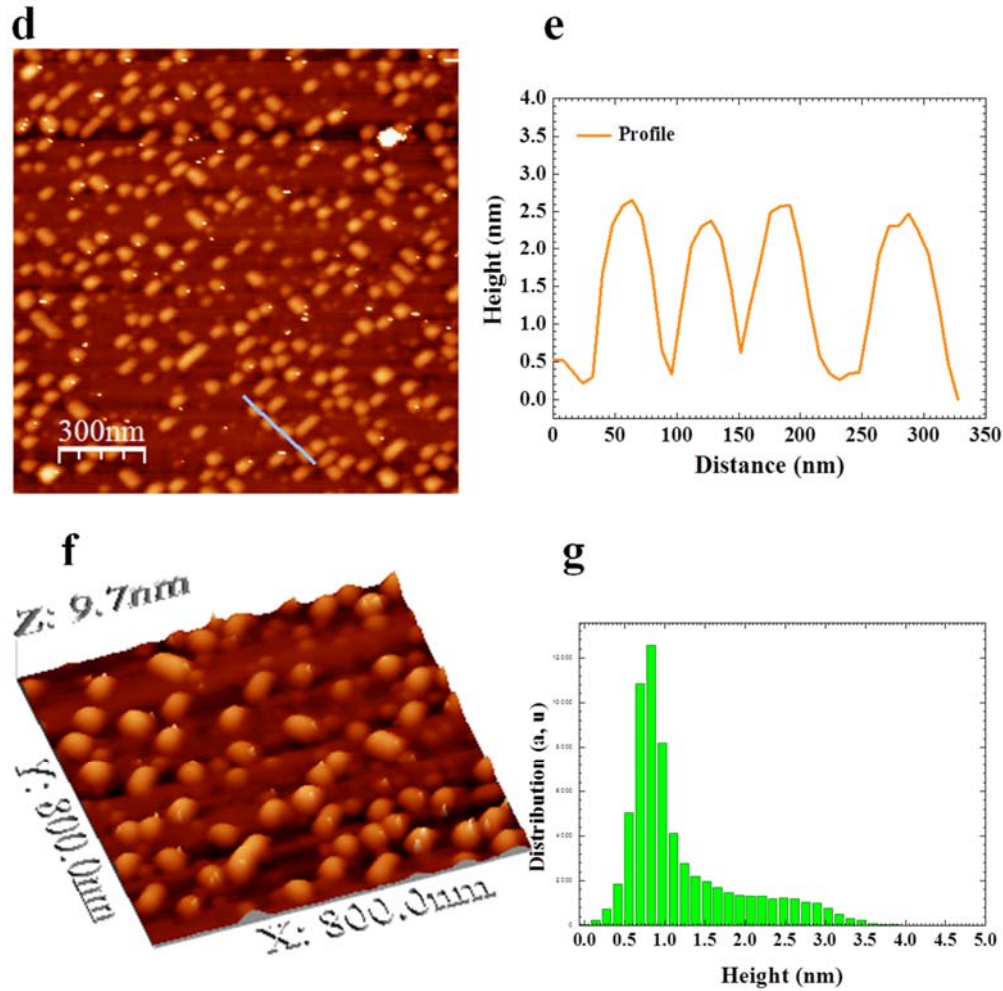


Figure 1. (a) and (b) show, respectively, the energy band diagram and a schematic representation of the fabricated  $p-i-n$  photodiode. (c) Display an AFM image of self-assembled GeMn quantum dots inserted in the  $p+i-n+$  photodiode's insulator layer. Figures (1-e) show the height profile along the line in (1-d)

### 3.2 Magnetic Characterization

Doping quantum dots with magnetic elements like Mn aims to exploit novel magnetic and electronic properties introduced by the transition chemical element (Mn) in Ge quantum dots to create high-performance devices like polarized light photodetectors or light-emitting diodes [15]. Furthermore, manganese can be used to tune the gap energy of nanocrystals and, as a result, tune the spectral response of tandem-type solar cells. The characterization of these quantum dots by SQUID showed that these GeMn quantum dots

are magnetic. Figure (2-a) shows the variation of the magnetization as a function of temperature ( $M$  vs.  $T$ ), and despite the small amount of GeMn deposited by MBE, the spectrum shows that the Curie temperature is approximately equal to 350 K. Figure (2-b) shows the variation of the magnetization as a function of the excitation field ( $M$  vs.  $H$ ). The  $M$ - $H$  characteristic is distinguished by a high remanence equal to  $4.5 \mu\text{emu}$  and a low coercivity equal to 400 Oe, allowing the spin in GeMn quantum dots to be easily manipulated using a weak excitation field. These magnetic properties show that these GeMn QDs are suitable for spin electronics and optoelectronics.

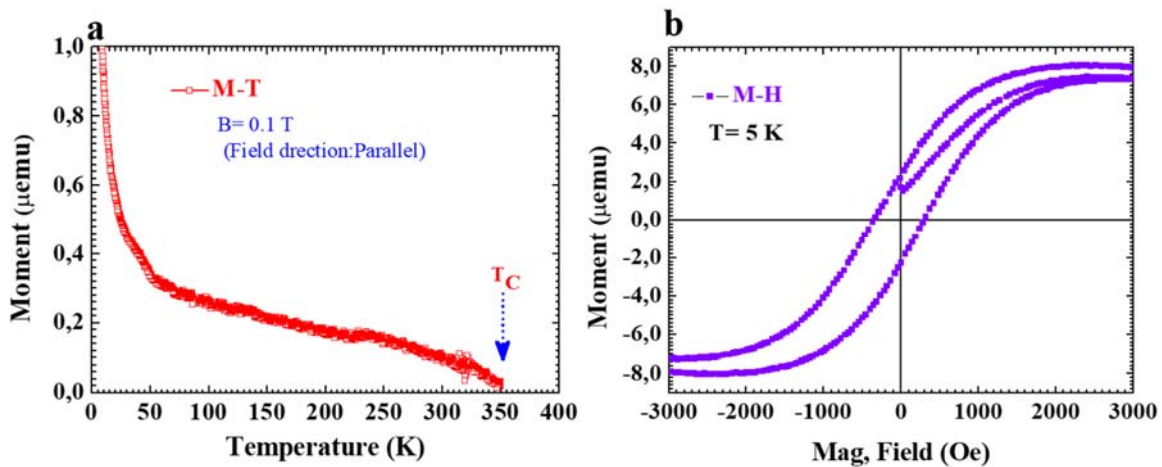


Figure 2.  $M(T)$  magnetization curve produced under a field of 0.1 T (a) and  $M(H)$  hysteresis cycle at  $T = 5$  K (b) of GeMn QDs epitaxied on Si (001).

### 3.3 Electrical Characterization

In order to study the electrical properties of the p<sup>+</sup>-i-n<sup>+</sup> photodiode, current density measurements as a function of voltage ( $J$ - $V$ ) and temperature were carried out using an HP 4140 B source meter and a station under cryogenic spikes. Figure 3 shows the  $J$ - $V$  characteristic measured at room temperature in the dark plotted on a linear scale (Figure 3-a) and on a logarithmic scale (Figure 3-b). Our structure's  $J$ - $V$  characteristic is typical of a p<sup>+</sup>-i-n<sup>+</sup> Schottky Barrier Diode (p<sup>+</sup>-i-n<sup>+</sup> SBD) with well-rectified behavior  $R = 10^7$ . The  $(\ln(J) -$

V) characteristic is linear on a semi-logarithmic scale, but for a large enough voltage, there is a deviation from this linearity due to the influence of series resistance and/or interface states.

Figure (3-c) shows the evolution of the (J-V) characteristics as a function of temperature. Under forward bias, these J-V plots shift to the higher bias side when temperature increases (Figure 3-d).

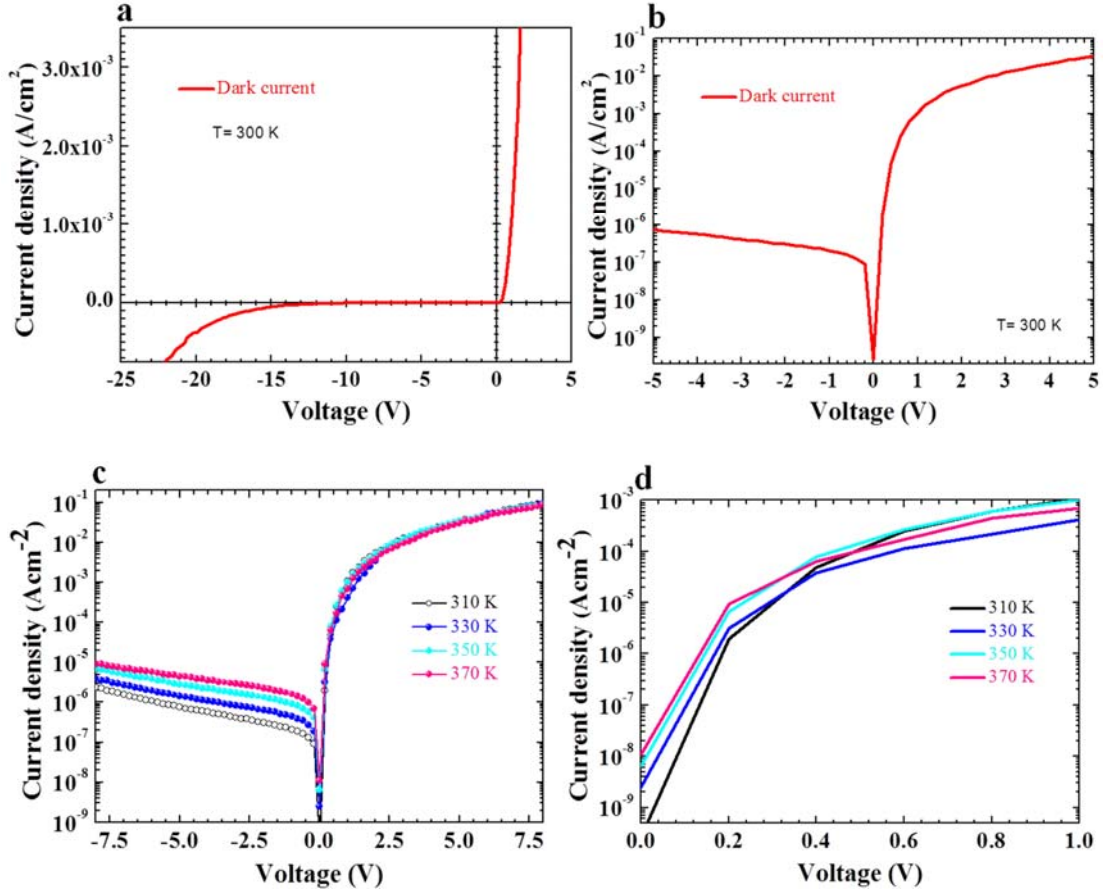


Figure 3. shows the J-V characteristic of a p+-i-n+ diode measured in the dark at room temperature and plotted in linear (a) and logarithmic scales (b).while Figure 3 (c and d) shows the (J-V) characteristics as a function of temperature.

To determine the value of the series resistance, the ideality factor, and the barrier height of a p+-i-n+ diode, we rely on the general theory of thermal emission. The transient current density of this diode is expressed by the relationship:

$$J = J_s \left[ \exp \frac{q(V - R_s J)}{nkT} - 1 \right] \quad (1)$$

Where  $S$  is the effective cross section of the diode,  $q$  is the elementary load,  $R_s$  is the series resistance of the diode,  $n$  is the ideality factor,  $k$  is the Boltzmann constant,  $T$  is the absolute temperature, and  $J_s$  is the saturation current density, which is written:

$$J_s = A^* T^2 \exp \frac{-q\phi_b}{kT} \quad (2)$$

Where  $A^*$  is the Richardson constant equal to  $112 \text{ cm}^{-2} \text{ K}^{-2}$  and  $\phi_B$  is the potential barrier.

For  $(V - R_s S J) \gg 3kT/q$ , relation (1) becomes:

$$J = J_s \exp \frac{q(V - R_s S J)}{nkT} \quad (3)$$

By calculating the parameters  $n$ ,  $\phi_B$ ,  $R_s$  with the Cheung and Cheung method [14], we can deduce the parameter responsible for the nonlinearity of the  $\ln(J)$ - $V$  characteristic. According to this method, we have:

$$\frac{dV}{d \ln(J)} = J S R_s + n \frac{kT}{q} \quad (4)$$

$$H(J) = V - \left( \frac{n k_B T}{q} \right) \ln \left( \frac{J}{A^* T^2} \right) \quad (5)$$

Where  $H(J)$  is written as:

$$H(J) = R_s S J + n \phi_B \quad (6)$$

The series resistance  $R_s$  can be extracted from the slope, and the ideality factor  $n$  and the height of the barrier can be extracted from the intersection with the ordinate axis. At room temperature, these values are  $R_s \approx 246 \Omega$ ,  $n = 1.86$  and  $\phi_B = 0.72 \text{ eV}$  respectively. Figure (4) shows the evolution of ideality factor and Schottky barrier height evolutions as functions of temperature for p<sup>+</sup>-Si/i-Si:GeMn QDs/n<sup>+</sup>-Si Schottky diode.

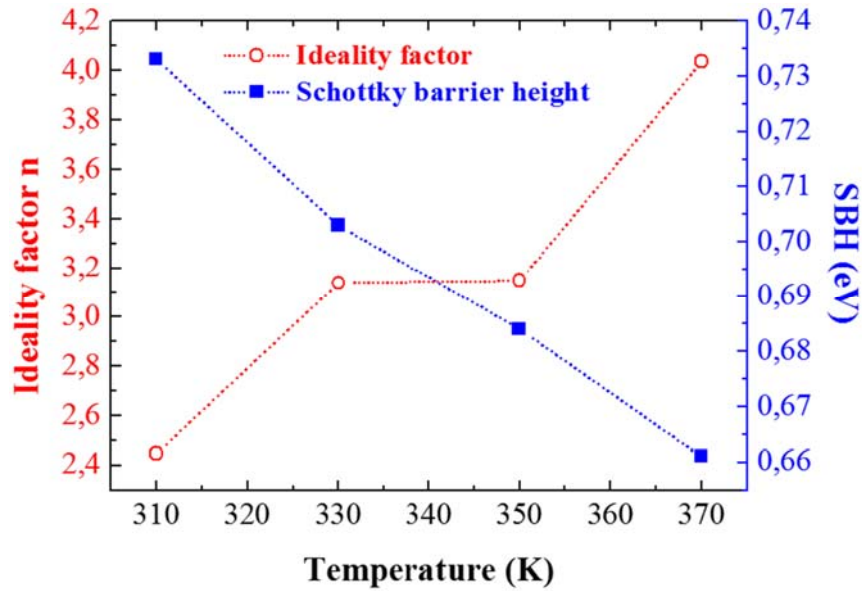


Figure 4. Show, ideally factor and Schottky barrier high evolutions as functions of temperature for  $p^+-Si/i-Si:GeMn$  QDs/ $n^+-Si$  Schottky diode.

The electronic transport mechanism in the Schottky diode is expressed through its ideality factor  $n$ : If  $n$  is close to 1, the diffusion current dominates the transport mechanism. For  $n$  between 1 and 2, it is the recombination effect that controls the current of the diode, which is the case for our structure. For  $n > 2$ , other effects come into play in the transport mechanism, such as tunneling, interface states, and the non-uniform distribution of interfacial charges.

Figures (5-a) and (5-b) show the experimental C-V and G-V characteristics, respectively, of the GeMn QDs- $p^+-i-n^+$  diode as a function of the bias voltage  $V_{DC}$  for different frequencies. The measurements were taken at room temperature using an HP4192 A LF type impedance analyzer equipped with an HP/Agilent 1 type test fixture specially designed to make high-precision impedance measurements. The  $V_{DC}$  voltage is superimposed with the AC excitation voltage ( $V_{AC}$  of 0.5 volts).

Figure 5-a shows that the capacitance of the GeMn QDs-PIN photodiode is very low; it is less than 2 pF. This low capacitance is desired for a  $p^+-i-n^+$  photodiode with high sensitivity and very high operational speed. For  $V_{DC} < 0.5$  V, a very low capacitance peak occurs (Fig. 5-a).

This peak can be attributed to the interface states that still exist in the p<sup>+</sup>-i-n<sup>+</sup> diodes. By increasing the frequency, this capacitance peak decreases and shifts towards low voltages, expressing a certain relaxation time of the component, which can be very important for the dynamic behavior of this diode. This phenomenon is attributed to the properties of the interface states. Beyond  $V_{DC} = 0.5V$ , the capacitance decreases and becomes independent of the frequency; this shows that this value of  $V_{DC}$  (0.5V) corresponds to the conduction threshold of the diode. This indicates that the photodiode has transitioned to the depletion region and is operating in full depletion mode at  $V_{DC} = 0.5 V$ .

Figure 5-b shows the variation of the conductance as a function of the voltage for the GeMn QDs-based p<sup>+</sup>-i-n<sup>+</sup> photodiode. The values of the conductance are high and of the order of 2 mS, unlike the capacitance, and remain almost constant as a function of the frequency as a function of the voltage from the polarization threshold  $V_{DC} = 0.5 V$ .

These results are similar to those of Wu and Yang [9]. Figures 5-c and 5-d show the variation of the capacitance and conductance of the p<sup>+</sup>-i-n<sup>+</sup> structure as a function of frequency for different bias values, respectively. The capacitance is very low, on the order of 2 pF, and remains almost constant as a function of the frequency and decreases slightly as a function of the voltage, which confirms the results obtained previously. The conductance of the p<sup>+</sup>-i-n<sup>+</sup> structure as a function of frequency is relatively high; it has a plateau at low frequencies of the order of 1  $\mu$ S and then increases at high frequencies. This increase is due to the fact that the charge trapping and detrapping processes can no longer keep up with the high frequencies of the AC signal.

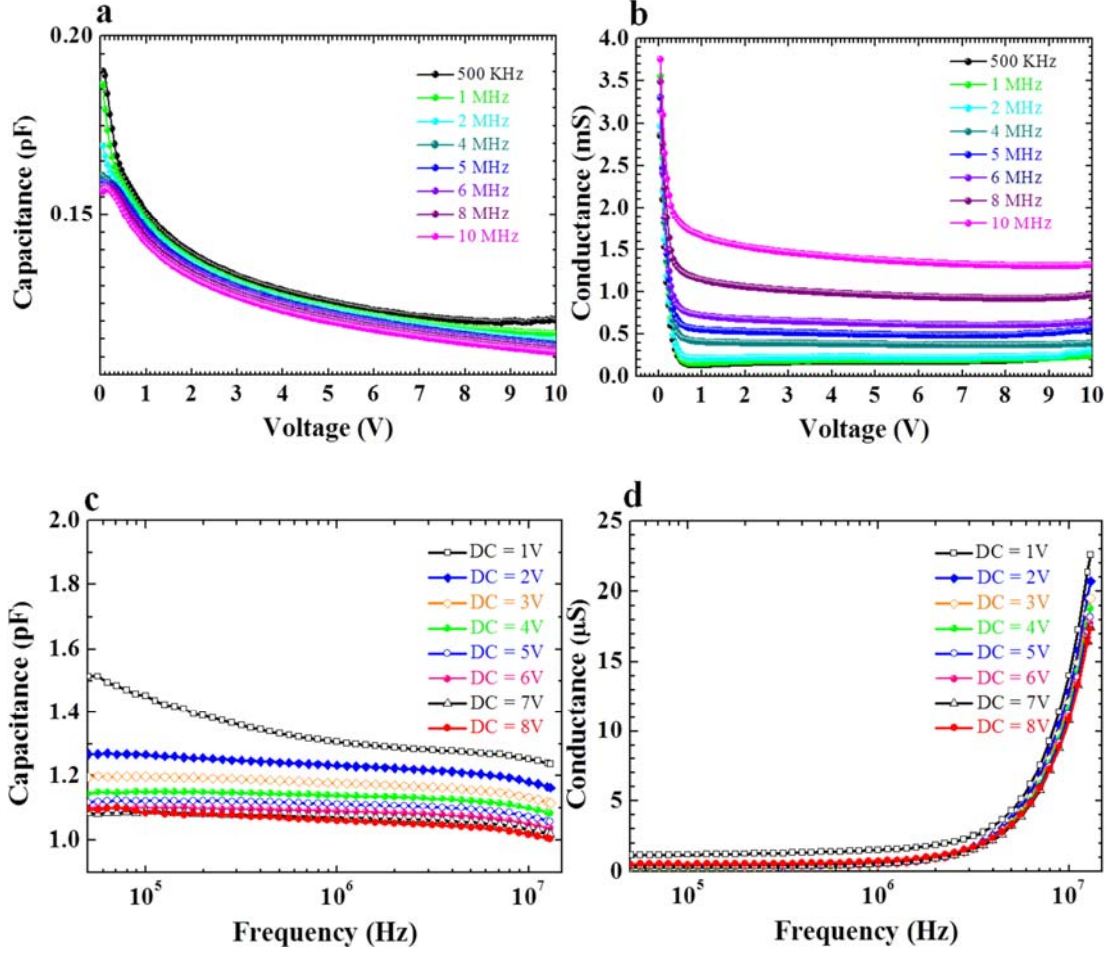


Figure 5. (a) and (b) show the C-V and G-V characteristics, respectively, of a Schottky diode at different frequencies; (c) and (d) show C-F and G-F characteristics at different biases (c and d), respectively, of a Schottky diode.

Under illumination at room temperature by white light from a halogen lamp incident on the circular aluminum contact (of radius 1 mm), the device produces a photocurrent density equal to  $6 \mu\text{A}/\text{cm}^2$  for a bias voltage  $V_b = -1 \text{ V}$ , which corresponds to the detector response of  $0.47\text{A}/\text{W}$ . This value is similar to that obtained by Wang [3] for a photodetector based on a pin photodetector with Ge QDs. Under the same conditions, the photosensitivity factor, defined as the ratio between the photocurrent and the dark current  $I_{\text{ph}}/I_{\text{dark}}$ , is  $10^2$  at a bias voltage  $V_b = -1\text{V}$ , indicating a strong response to white light.

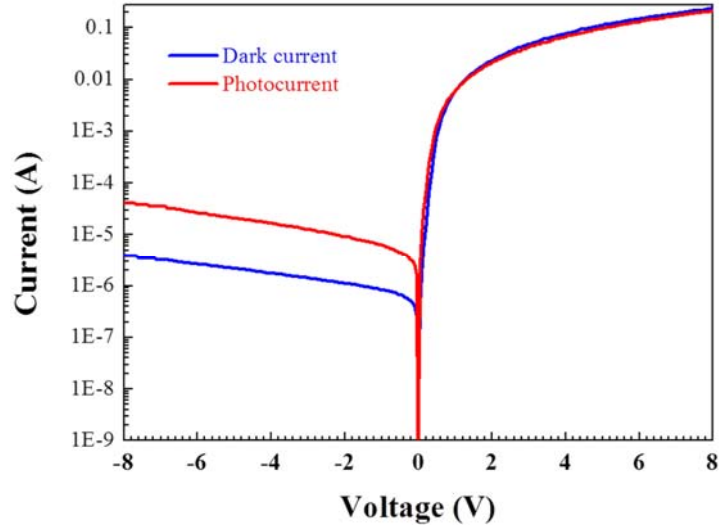


Figure 6. *J-V characteristics of p+-i-n+ diode measured in the dark and under illumination at room temperature.*

By comparing these results with the results reported in the literature on a p+-i-n+ diode with Ge quantum dots without manganese doping, we find that our p+-i-n+ diode with GeMn quantum dots has more improved electrical properties, especially at the level of the breakdown voltage and the height of the Schottky barrier height; indeed, our diode shows a breakdown voltage of -12 V and a value of the Schottky barrier height of 0.72 eV at room temperature; these two values are higher compared to those reported in the literature [3, 16]. Moreover, our p+-i-n+ diode with GeMn QDs is superior to other p+-i-n+ diode with its unique magnetic properties, which increases its importance in advanced applications. All these results testify to the high quality of the structure and the molecular beam epitaxy reactor that we used to fabricate the device.

### 3.4 Photocurrent Spectroscopy

The spectral operating range of the p+-i-n+ photodetector with GeMn QDs was determined by measuring the photocurrent generated by the pin diode as a function of the wavelength, which varies from ultraviolet to visible, by illuminating the photodiode with a tunable

monochromatic light beam produced using a monochromator and a halogen lamp. The light beam is amplitude modulated by an optical chopper at a frequency of 200 Hz to eliminate the noise signal, and the photocurrent signal produced by the diode is collected and filtered using synchronous detection.

The spectra of the photocurrent produced by the pin photodiode (Figure 7) show that the spectral response has a wide band in the visible range with a peak of the maximum photocurrent located at 700 nm; this peak is attributed to the germanium quantum dots. The shift of this peak from the infrared to the visible is due to the quantum confinement in the GeMn quantum dots. This means that the spectral response is tunable in wavelength via the degree of confinement chosen in the GeMn QDs because the detector only reacts to light whose energy is greater than the gap energy of the quantum boxes of GeMn. Furthermore, the visible response of these quantum boxes shows that manganese-doped Ge boxes have a potential application for solar cells since, on the one hand, they are compatible with the technology of silicon-based solar cells and, on the other hand, there is a visible response, or the intensity of the solar spectrum is very strong.

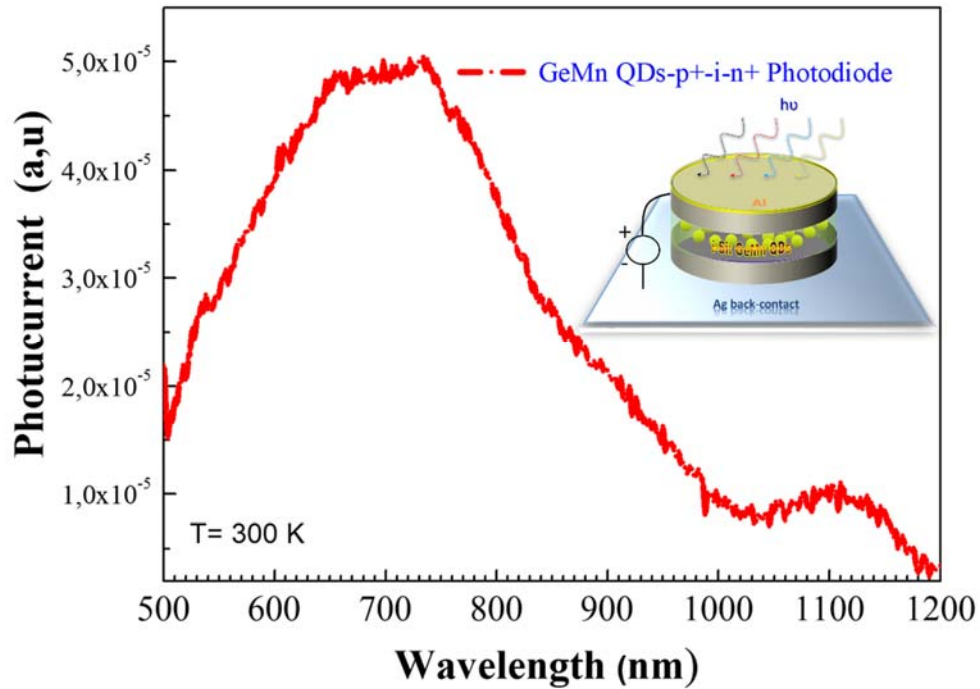


Figure 7. The spectral response of  $p^+-i-n^+$  Photodiode with GeMn QDs at room temperature.

#### 4. Conclusion

A  $p^+-i-n^+$  photodetector based on germanium quantum dots doped with manganese has been demonstrated. The germanium quantum dots with a low percentage of Mn are monolithically grown by MBE via the Stranski-Krastanov mode. The GeMn quantum dots exhibit Curie temperatures higher than room temperature ( $T_C = 350$  K), a high remanent magnetization of  $4 \mu\text{emu}$ , and a low coercivity of  $500$  Oe. The electrical measurements indicate that the  $p^+-i-n^+$  photodetector with GeMn QDs has a Schottky barrier height and an ideality factor that were evaluated to be  $0.72$  eV and  $1.86$ , respectively, at  $300$  K. Capacitance and conductance measurements show that the photodetector has a very low interface state density which allows the photodetector to start operating in full depletion mode for low bias voltage ( $V_b = -0.5$  V) which allows to reduce the consumption of energy when it is on. The GeMn QDs-based  $p^+-i-n^+$  photodetector have response spectral in the visible with a high sensitivity of the order of

100. These original results pave the way for the real integration of dilute magnetic nanostructures in advanced optoelectric applications.

**Acknowledgement:**

This work was funded by the Deanship of Scientific Research at Jouf University under grant No (DSR-2022-RG-0138).

**References:**

- (1) P. Olsson, J-F. Guillemoles and C. Domain, *J. Phys.: Condens. Matter.* 20 (2008) 064226.
- (2) M.L. Lee, F.W. Huang, P.C. Chen, J.K. Sheu. *Sci Rep.* 8 (2018) 8641.
- (3) U.M. Kannan, L. Giribabu, S. Narayana Jammalamadaka. *Solar Energy.* 187 (2019) 281-289.
- (4) A. Gouye, I. Berbezier, L. Favre, G. Amiard, M. Aouassa, Y. Campidelli, A. Halimaoui. *Applied Physics Letters.* 96 (2010) 063102.
- (5) M. Aouassa, A. Ronda, L. Favre, A. Delobbe, P. Sudraud, I. Berbezier, *Journal of Applied Physics.* 114 (2013) 034301.
- (6) A. Gouye, I. Berbezier, L. Favre, M. Aouassa, G. Amiard, A. Ronda, Y. Campidelli, A. Halimaoui. *Journal of Applied Physics.* 108 (2010) 013513.
- (7) M. Aouassa, L. Hassayoun, L. Favre, et al.. *J Mater Sci: Mater Electron.* 30 (2019) 2585–2591.
- (8) M. Aouassa, I. Jadli, L. S. Hassayoun, H. Maaref, G. Panczer, L. Favre, A. Ronda, I. Berbezier. *Superlattices and Microstructures.* 112 (2017) 493-498.
- (9) M. Aouassa, I. Jadli, M. A. Zrir, H. Maaref, R. Mghaieth, L. Favre, A. Ronda, I. Berbezier. *Journal of Porous Materials.* 24 (2017) 1139-1144.
- (10) V. Zhandun, A. Matsynin, *Chinese Journal of Physics.* 68 (2020) 9-18.
- (11) N. Stojilovic, S. V. Dordevic, Rongwei Hu, and C. Petrovic. *J. Appl. Phys.* 114 (2013) 053708.

- (12) M. Aouassa, I. Jadli, A. Bandyopadhyay, S. K. Kim, I. Karaman, J. Y. Lee, *Applied Surface Science*. 397 (2017) 40-43.
- (13) Matioli, E., Brinkley, S., Kelchner, K. *et al.* High-brightness polarized light-emitting diodes. *Light Sci Appl* **1**, e22 (2012). <https://doi.org/10.1038/lssa.2012.22>.
- (14) S. K. Cheung and N. W. Cheung ; *Applied Physics Letters* 49 (2):85 – 87;  
DOI:10.1063/1.97359.
- (15) Shen, L., Zhang, X., Wang, J. *et al.* Mn-doped SiGe thin films grown by UHV/CVD with room-temperature ferromagnetism and high hole mobility. *Sci. China Mater.* **65**, 2826–2832 (2022). <https://doi.org/10.1007/s40843-022-2025-x>.
- (16) M. Oehme, A. Karmous, M. Sarlija, J. Werner, E. Kasper, and J. Schulze; Ge quantum dot tunneling diode with room temperature negative differential resistance; *APPLIED PHYSICS LETTERS* 97, 012101 (2010).